13th International Conference on Greenhouse Gas Control Technologies, GHGT-13, 14-18 November 2016, Lausanne, Switzerland

Raman Spectroscopy as an Online Monitoring Tool for CO2 Capture Process: Demonstration Using a Laboratory Rig

M.H. Wathsala N. Jinadasa, Klaus-J. Jens, Lars Erik Øi, Maths Halstensen*

Faculty of Technology, University College of Southeast Norway, 3918, Porsgrunn, Norway

Abstract

A laboratory CO2 capture rig at USN was used as a demonstration plant to show the feasibility of Raman spectroscopy for online monitoring of speciation in CO2 capture process. The spectroscopy was integrated to lean and rich amine streams and experiments were carried out in dynamic and steady state conditions. Multivariate models were used to predict the speciation with time. Predicted CO2 and MEA concentrations were compared with offline analysis and the ion speciations were compared with a thermodynamic model. Results indicated that the Raman spectroscopy together with chemometrics based approach is an effective tool for online monitoring of speciation.

Keywords: CO2 capture, Raman spectroscopy, partial least square regression, multivariate data analysis, online speciation

1. Introduction

According to IEA Technology Roadmap 2013[1], the next step for many CO2 capture technologies is to move to demonstration scale by 2020. Successful demonstration criteria should include online monitoring and real time analysis where the need of process analytical methods such as infrared, Raman and nuclear magnetic resonance spectroscopy will become an integral part in CO2 capture plants in near terms. There is an emerging research interest of using these analytical techniques from lab to industrial scale as online monitoring tools for speciation in

---

* Corresponding author. Tel.: +47 35575187; fax: +47 35575001.
  E-mail address: maths.halstensen@hit.no

MEA-CO2-H2O system ([2-4]). Raman spectroscopy is a powerful Process Analytical Technology (PAT) and its feasibility for fast response, remote sampling and water-independent spectral features, make it a possible candidate for online applications in CO2 capture process than IR spectroscopy or NMR spectroscopy. The Raman phenomenon is based on vibrational changes of Raman scattered electromagnetic radiation. Previous studies [5-7] show that the Raman signal is highly rich with chemical information on carbon and amine species. However, converting Raman spectra into chemical information requires data pre-processing prior to interpretation and quantification. Raman intensity is always a combination of noise and chemical signal due to changes of baseline and peak overlaps and may result in erroneous data interpretation. Chemometrics is a multivariate analysis approach which is often preferred to deal with these spectral challenges and is used to calibrate reliable prediction models [8]. In PAT applications, widely used chemometrics method for regression modelling is partial least square regression (PLSR). The output of a PAT instrument comes with hundreds of wavenumbers which are more or less important with the measured property. Using PLS method, x variables (wavenumbers) are correlated with y variable (measured property), such that covariance between x and y are maximized.

This study is the second step of ongoing research at University College of Southeast Norway (USN) to enable Raman spectroscopy for industrial scale CO2 capture process. In the first step, Raman and multivariate based PLS models were calibrated and validated for complete speciation analysis of CO2 absorption process based on lab scale experiments. Measurements were taken at equilibrium conditions. In the second step, which is described in this paper, the models were assessed in terms of predictability and robustness in insitu application.

1.1. Chemistry and speciation

Reaction of aqueous alkanolamines with carbon dioxide involves an acid–base buffer mechanism where it finally forms a large number of carbon species and amine species in the liquid phase. The equilibrium reactions can be written as shown in (1) to (6).

$$H_2O + H_2O \Leftrightarrow H_3O^+ + OH^- \tag{1}$$

$$CO_2 + H_2O \Leftrightarrow H_2CO_3 \tag{2}$$

$$H_2CO_3 + H_2O \Leftrightarrow HCO_3^- + H_3O^+ \tag{3}$$

$$HCO_3^- + H_2O \Leftrightarrow CO_3^{2-} + H_3O^+ \tag{4}$$

$$R_1R_2NH + H_3O^+ \Leftrightarrow R_1R_2NH_2^+ + H_2O \tag{5}$$

$$2R_1R_2NH + CO_2 \Leftrightarrow R_1R_2NCOO^- + R_1R_2NH_2^+ \tag{6}$$

Overall mass balance for amine species in the solution can be defined as the summation of protonated amine, carbamate and free amine (7) while that for carbon species is the sum of bicarbonate, carbonate and molecular CO2 (8).

$$C_{MEA\ total} = C_{MEA+} + C_{MEACOO^-} + C_{free\ MEA} \tag{7}$$

$$C_{total\ CO2} = C_{HCO_3^-} + C_{MEACOO^-} + C_{CO_3^{2-}} + C_{CO2} \tag{8}$$

Thermodynamic property models related to MEA-CO2-H2O systems represent vapor-liquid equilibrium (VLE) and they are extensively used in process design and optimization. Kent and Eisenberg model [9], Deshmukh and Mather Model [10] and electrolyte nonrandom-two-liquid (NRTL) model[11] are some of such models referred in CO2 capture research.

2. Experimental section

2.1. CO2 rig at USN

The rig consists of an absorption column with an inner diameter of 0.1 m and height of 2.5 m. Desorption column has an inner diameter of 0.26 m, a packing height of 1 m with a steam heated reboiler. The maximum liquid circulation and gas flow rates are 250 kg/h and 40 Nm3/h respectively. Fig. 1 shows the process flow diagram of the rig. A buffer tank is located between the absorber and the desorber. Liquid is loaded to the buffer tank before the circulation begins and synthetic CO2 is fed to the system by mixing with an air supply to the required volumetric ratio. Locations of Raman sensors, T1/T2 temperature sensors and nondispersive infrared sensor (NDIR) for CO2 gas measurement are shown in the figure. Two manual sampling valves are located soon after the Raman flow cells to extract samples for offline analysis.
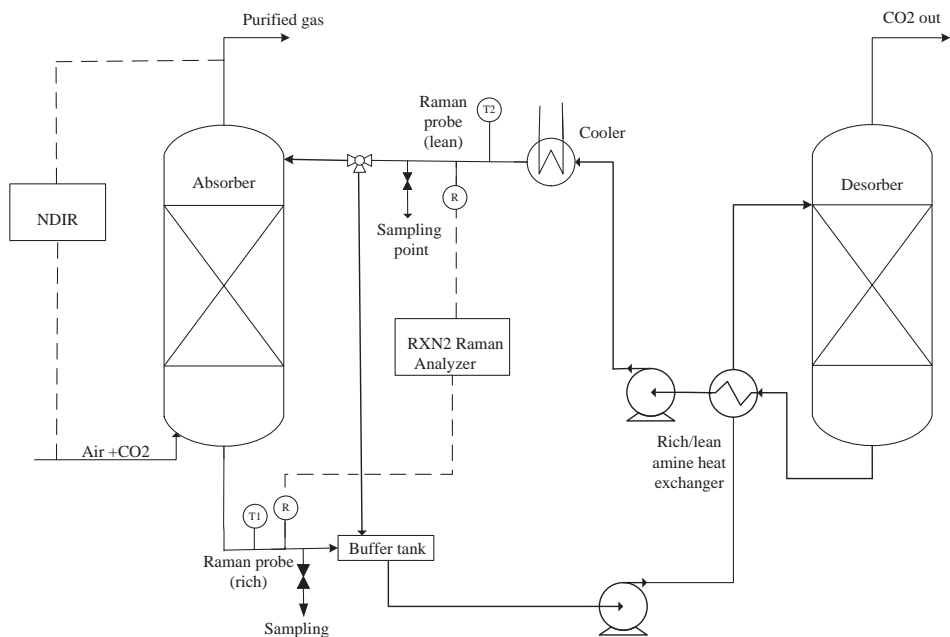

(a). Process flow diagram of CO2 rig
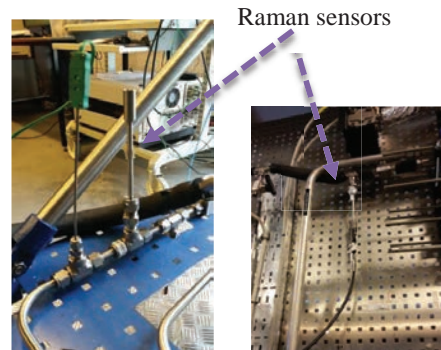
(b) Picture of CO2 rig   *(c) Raman sensor locations ; rich stream (left), lean stream (right)*

Fig. 1: Layout of USN CO2 rig (R=Raman sensor; T=Temperature sensor)

2.2. Instruments and chemicals

RXN2 portable multichannel Raman spectrometer (Kaiser Optical Systems Inc.) was the newly integrated system to the rig. The instrument is equipped with NIR dioder laser with wavelength of 785 nm spanning in the spectral range of 100–3425 cm-1. Four fiber optic probes can be connected and utilized through an automatic sequential scanning system that is integrated into the instrument. The Raman spectra were acquired using a short-focus (200 µm)-sapphire-window- Hastelloy probe optic which should be in direct contact with a solution. 99% MEA solvent purchased from VWR was used for the rig experiments. 0.1M Sodium hydroxide (NaOH), 0.1 M hydrochloric acid (HCl) and 1 M HCl purchased from Merck were used for the titration experiments. Titrator Mettler Toledo T50, were used for determining pH, CO_2 loading and MEA concentration.

2.3. PLSR models and predictions

There are six PLSR models developed using different CO_2 loaded 30% MEA equilibrium samples at room temperature and pressure. The aim of these models were to enable Raman spectroscopy to use as an analytical method for speciation of MEA-CO_2-H_2O system. Five out of these models can predict the species of carbonate, bicarbonate, carbamate, protonated amine and free amine and the remaining one can predict the total CO_2 loading. 23 calibration and 22 validation samples were used for the model development. Quantitative analysis of species distribution for each sample was performed by ^{13}C NMR experiments. Raman spectra were collected, smoothed and important wavenumbers were cropped based on the prior knowledge on their characteristic Raman bands. They were then regressed with respect to the species concentrations (y variable) in Matlab PLS toolbox to develop PLS models. Table 1 summarises the results of these models for 6 constituents including the range and root mean square error of prediction (RMSEP). The definition of RMSEP is given in (9) where $y_{predicted}$ is the predicted value from the PLSR model, $y_{reference}$ is the measured value and I is the number of samples in the validation data set.

Table 1 : Summary of 6 PLSR models

Species	Range $\pm$ RMSEP
CO_2 loading (mol CO_2 / mol MEA)	$(0.0 – 0.49) \pm 0.0109$
Carbonate (mol / kg H_2O)	$(0.0 – 0.09) \pm 0.0033$
Bicarbonate (mol / kg H_2O)	$(0.0 – 1.33) \pm 0.0519$
Carbamate (mol / kg H_2O)	$(0.0 – 3.08) \pm 0.0565$
MEAH+ (mol / kg H_2O)	$(0.0 – 3.9) \pm 0.054$
Free amine (mol / kg H_2O)	$(0.0 -5.8) \pm 0.236$

$$RMSEP = \sqrt{\frac{\sum_{i=1}^{I}\left(y_{predicted} - y_{reference}\right)^2}{I}} \qquad (9)$$

These PLSR models can be used to predict the species concentrations in future MEA-CO_2-H_2O samples based on their Raman spectra.

2.4. Screening experiments – model validation

Tasks carried out in this research are twofold. First set of experiments were meant to assess the validity of the PLSR models against offline measurements while the second set was aimed at demonstrating the model capacity in dynamic process situations.

Table 2 : Description of process conditions in screening experiments – model validation

Run No:	Day	Time	CO2 in (vol%)	CO2 out (vol %)	Gas flow (Nm3/h)	Liquid flow (kg/h)	T1 (^{0}C)	T2 (^{0}C)	Boiler temperature (^{0}C)	CO2 removal efficiency
1	Day 1	11.41	9.9	0.7	5	39	46	39	120	0.93
2		11.52	10	2.8	10	39	40	39	120	0.72
3		12.02	10.1	4.8	15	33	32	37	120	0.52
4		12.18	9.9	6.1	20	40	27	38	119	0.38
5		12.31	10	6.9	25	40	24	39	119	0.31
6		12.43	10	7.3	30	40	22	37	120	0.27
7	Day 2	11.03	9.9	5.2	30	114	38	38	119	0.47
8		11.37	9.8	5.8	30	100	35	38	118	0.41
9		11.46	9.9	5.8	30	88	33	39	118	0.41
10		12.06	10.2	6.5	30	100	31	38	117	0.36
11		12.22	10.1	6.6	30	70	29	39	117	0.35
12		12.37	-	-	30	60	24	38	117	-
13	Day 3	11.41	10	5.2	20	112	37	33	117	0.48
14		11.55	10.2	5.36	20	100	38	38	117	0.47
15		12.10	9.8	5.4	20	90	38	39	117	0.45
16		12.27	10.1	5.23	20	80	37	39	118	0.48
17		12.44	10	5.55	20	70	35	39	118	0.44
18		12.57	9.9	5.7	20	60	41	34	118	0.42
19		13.09	9.9	5.9	20	50	31	36	118	0.40
20		13.26	9.8	6.1	20	40	27	37	118	0.37
21		13.37	9.8	6.8	20	30	23	37	119	0.30
22	Day 4	11.22	10.2	4.4	20	110	42	39	119	0.59
23		11.38	10.1	4.4	20	100	41	40	119	0.57
24		11.58	10.2	5	20	90	40	40.	119	0.54
25		12.23	10	5	20	80	37	40	118	0.5
26		12.46	10.1	5.7	20	70	35	39	118	0.45
27		13.04	10.2	5.7	20	60	33	39	119	0.44
28		13.27	9.9	6.3	20	50	31	39	119	0.41

In the *'model validation'* experiments, the rig was operated for 4 days changing liquid flow rates (30 - 115 kg/h) and gas flow rates (5-20 Nm^3/h). The absorber liquid inlet temperatures was set to 40^{0}C and the CO2 content to the absorber was maintained at 10 vol-% to allow sufficient CO2 to react with MEA. Raman spectra were acquired in 1 minute intervals by the Raman analyser and automatically imported to Matlab/Labview interface where further signal processing was done and selected Raman wavenumbers were exported to perform PLSR model predictions. Only one Raman probe was used during these experiments except for run 1-6. At certain times, 28 liquid samples were collected manually from the sampling points located adjacent to each Raman probe locations for offline measurements.

Key process conditions of the test rig during 4-day trials are given in Table 2. Run 1-6 was related to increasing the gas flow from 5 to 30 Nm^3/h while maintaining the liquid flow at 40 kg/h. In Run 7-12, liquid flow was decreased from 115 to 60 kg/h while keeping gas flow constant at 30 Nm^3/h. Run 13-21 and 22-28 are similar trials where liquid flow was decreased from 115 to 30 kg/h while keeping gas flow constant at 20 Nm^3/h. CO2 removal efficiency calculated based on gas flow measurements by NDIR is also included in Table 2.

2.5. Screening experiments – demonstration

The purpose of screening experiments-demonstration was to see the effect of dynamic process conditions to the model predictions. The easily controllable process conditions of the rig were gas flow rate, liquid flow rate, CO2 % in flue gas and absorber inlet temperature. CO2 concentration in the rich and lean streams was expected to vary in the range of 0-0.45 when the above conditions were varied. Variations of MEA concentrations were also expected due to the water loss at high temperatures of the desorber operation. Four demonstration cases were defined with

varying process conditions as shown in Table 3. Only one case was run per day and each case was around 2.5 hour duration.

Table 3: Description of process conditions in screening experiments – demonstration ((*reg = regeneration in the desorber))

Experiment	Gas flow rate (Nm³/h)	Liquid flow rate (kg/h)	CO2 v/v% in flue gas	Desorber condition	lean loading	rich loading
Case 1	4	200	4	without reg*.	0.03-0.06	0 .03-0.06
Case 4	4	200	0	with reg.	0.25-0.28	0.25-0.28
Case 1	4	150	0	without reg.	0.03-0.06	0 .03-0.06
Case 1	4	80	4	without reg.	0.03-0.06	0 .03-0.07
Case 3	4	30	10	with reg.	0.22-0.43	0.37-0.44
Case 1	14	200	4	without reg.	0.03-0.1	0.04-0.1
Case 2	14	150	10	without reg.	0.2-0.33	0.2-0.36
Case 3	14	150	11	with reg.	0.36-0.42	0.36-0.42
Case 2	14	150	0	without reg.	0.3-0.32	0.3-0.32
Case 3	14	150	0	with reg.	0.36-0.38	0.36-0.38
Case 4	14	150	0	with reg.	0.17-0.28	0.17-0.28
Case 1	14	80	4	without reg.	0.03-0.06	0.15-0.18
Case 4	14	80	4	with reg.	0.24-0.25	0.3-0.38
Case 4	14	80	10	with reg.	0.24-0.28	0.26-0.38
Case 1	14	30	4	without reg.	0.03-0.06	0.03-0.1
Case 4	14	30	10	with reg.	0.18-0.19	0.4-0.44
Case 3	14	30	10	with reg.	0.22-0.24	0.41-0.44
Case 1	30	200	4	without reg.	0.08-0.12	0.08-0.12
Case 1	30	200	10	without reg.	0.21-0.26	0.24-0.29
Case 1	30	150	4	without reg.	0.12-0.14	0.13-0.16
Case 1	30	150	10	without reg.	0.17-0.23	0.24-0.26
Case 3	30	150	11	with reg.	0.35-0.38	0.32-0.35
Case 1	30	80	4	without reg.	0.13-0.16	0.18-0.29
Case 1	30	80	10	without reg.	0.14-0.19	0.25-0.42
Case 1	30	30	4	without reg.	0.12-0.14	0.26-0.29
Case 1	30	30	10	without reg.	0.13-0.15	0.40-0.43
Range (for all the cases)	4-30	30-200	0-10		0.03-0.43	0.03-0.44

3. Results and discussion

A CO2 loaded MEA sample produces a Raman spectrum with several bands from 300 to 1700 cm-1, a broad area from 1700 to 2700 cm-1 and a couple of sharp overlapped bands from 2850 to 3050 cm-1 as illustrated in Fig. 2. Characteristic Raman bands and vibrational assignments of the species that were found in liquid phase of unloaded MEA and CO2 loaded aqueous MEA during this study are given in Table 4. All the Raman bands identified in CO2 loaded 30% MEA samples at equilibrium conditions in the calibration and validation set used for PLSR models could be identified in the Raman signals acquired during this online study.
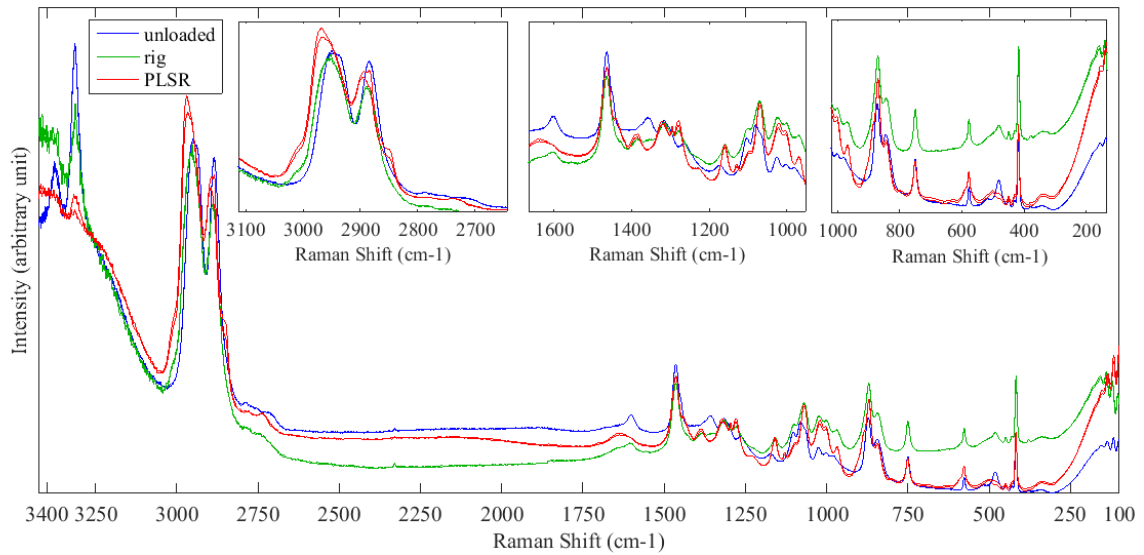
Fig. 2 : Comparison of Raman signals for CO2 loaded and unloaded MEA

Table 4: Vibrational assignments of species in MEA-CO2-H2O system

Specie	Frequency (cm-1)	Frequency (cm-1) (Literature)	Vibrational mode [reference]	Bands identified in		
				CO2 unloaded 30% MEA samples	calibration and validation samples - PLSR	lean and rich amine streams in USN rig
MEA	417	417	CC deformation [12]	√	√	√
	481	481	CC deformation [12]	√	√	√
	843	845	CH2 rocking + CN stretching [13]	√	√	√
	871	873	CH2 rocking + CN stretching [13]	√	√	√
	1029	1030	CN stretching [14]	√	√	√
	1464	1460	CH bend [14]	√	√	√
	2885	2870	CH2 symmetric stretch [14]	√	√	√
	2934	2930	CH2 asymmetric stretch [14]	√	√	√
MEACOO$^-$	1160	1155	C N stretching [15]		√	√
MEAH+	1277	1274	N-CH stretch [16]		√	√
	1320	1320	CC stretch [16]		√	√
	2894	2700-3000	NH$_2$+ stretching [12]		√	√
	2975	2700-3000	NH$_2$+ stretching [12]		√	√
CO32-	1070	1065	Symmetric CO stretching [17]		√	√
	1385	1380	Antisymmetric CO stretching [17]		√	√
HCO3 -	1024	1017	C-OH stretching [17]		√	√
CO2	1278	1274	CO2 symmetric stretch + CO2 bend overtone [14]		√	√
	1389	1383	CO2 Symmetric stretch + CO2 bend overtone [14]		√	√

The comparison of Raman bands between CO2 loaded samples and unloaded amine samples give an indication about the newly appeared Raman bands due to the CO2 absorption by amine.

3.1. Screening experiments – model validation

Based on the equilibrium or non-equilibrium conditions, variations of different CO_2 loadings and amine concentration with time was expected in the CO_2 rig operation. According to the experimental conditions stated for run 1-28 in Table 2, the behavior of model predictions in such dynamic environment was assessed. By applying six PLSR models, species concentrations of each run were predicted using Matlab PLS toolbox and results are shown in Table 5. 28 runs given in Table 5-1 corresponds to the same run number in Table 2. From the results presented in Table 5-1 and 5-2, total CO_2 loading determined from offline titration measurement can be compared with the CO_2 loading – PLS model predictions as well as the summation of carbonate-bicarbonate-carbamate – PLS models. In run number 8-L and 20-R, predictions highly deviate from the rest of runs and this was assumed due to an instrument noise. The difference between the CO_2 loading – PLS model and the summation of PLS predictions by three carbon species (carbonate + bicarbonate + carbamate) was assumed to be equal to the molecular CO_2 which had not reacted with amine. This difference was higher in rich stream than the lean stream as rich stream Raman measurement point was located very close to the CO_2 inlet to the absorber and hence more CO_2 could exist in aqueous level. Less quantitative difference between column 1 and 9, is an indication of the validity of CO_2 loading – PLS predictions.

Table 5-1 : Speciation results from 28 runs;
(Uc = uncertainties calculated by Matlab Toolbox(Uc = uncertainties calculated by Matlab Toolbox)

			Predictions from PLSR models					
			Column 1	Column 2	Column 3	Column 4	Column 5	Column 6
Run no:	Day	Time (L=lean; R= rich)	CO_2 loading ± Uc[*] (mol / mol MEA)	Carbonate ± Uc (mol / kg H2O)	Bicarbonate ± Uc (mol / kg H2O)	Carbamate ±Uc (mol / kg H2O)	MEAH+ ± Uc (mol / kg H2O)	Free MEA ± Uc (mol / kg H2O)
1	Day 1	11:41 - R	0.3319 ± 0.0173	0.049± 0.006	0.041± 0.021	2.352± 0.143	2.50± 0.24	2.28± 0.36
3		12:02 - R	0.4118 ± 0.0176	0.065± 0.007	0.055± 0.021	2.706± 0.144	2.81± 0.22	1.63± 0.38
6		12:43 - R	0.4290 ± 0.0178	0.069± 0.007	0.057± 0.022	2.793± 0.144	2.86± 0.22	1.47± 0.39
1		11:41 - L	0.2244± 0.0174	0.030± 0.007	0.011± 0.021	1.437± 0.146	1.39± 0.23	4.19± 0.41
3		12:02 - L	0.2361± 0.0174	0.028± 0.007	0.021± 0.021	1.297± 0.148	1.40± 0.21	4.35± 0.42
6		12:43 - L	0.2591± 0.0173	0.038± 0.007	0.023± 0.021	1.465± 0.146	1.97± 0.28	3.97± 0.40
8	Day 2	11:37 - R	0.2345± 0.0175	0.034± 0.006	0.029± 0.020	1.519± 0.150	2.38± 0.32	2.94± 0.37
10		12:06 - R	0.4066± 0.0179	0.066± 0.007	0.056± 0.021	2.291± 0.151	2.82± 0.22	2.00± 0.38
12		12:37 - R	0.4436± 0.0173	0.079± 0.008	0.072± 0.021	2.432± 0.147	3.72± 0.36	1.84± 0.37

8		11:37 - L	0.2774± 0.0174	0.106± 0.015	0.108± 0.034	0± 0.406	3.20± 0.71	6.38± 0.54
10		12:06 - L	0.2850± 0.0173	0.041± 0.006	0.031± 0.020	2.119 0.143	2.12± 0.23	2.81± 0.39
12		12:37 - L	0.3075± 0.0173	0.049± 0.006	0.039± 0.020	2.093± 0.143	2.38± 0.23	2.84± 0.39
14	Day 3	11:55 - R	0.3985± 0.0176	0.065± 0.006	0.064± 0.021	2.628± 0.144	2.51± 0.26	1.79± 0.41
16		12:27 - R	0.3111± 0.0175	0.047± 0.007	0.045± 0.020	1.893± 0.145	2.23± 0.26	2.99± 0.36
18		12:57 - R	0.2849± 0.0176	0.045± 0.006	0.045± 0.020	1.911± 0.143	2.10± 0.24	3.09± 0.37
20		13:26 - R	0.3832± 0.0178	0.089± 0.010	0.122± 0.030	0± 0.442	3.19± 0.78	7.07± 0.59
14		11:55 - L	0.4221± 0.0173	0.068± 0.007	0.070± 0.021	2.761± 0.144	2.59± 0.25	1.71± 0.39
16		12:27 - L	0.2805± 0.0173	0.044± 0.006	0.051± 0.021	0.515± 0.267	3.21± 0.66	4.62± 0.41
18		12:57 - L	0.2604± 0.0173	0.040± 0.006	0.036± 0.020	1.742± 0.144	1.86± 0.25	3.54± 0.38
20		13:26 - L	0.4360± 0.0173	0.072± 0.007	0.068± 0.021	2.869± 0.145	2.83± 0.25	1.40± 0.42
23	Day 4	11:38 - R	0.3424± 0.0174	0.055± 0.006	0.055± 0.021	2.321± 0.143	2.46± 0.22	2.18± 0.39
25		12:23 - R	0.2232± 0.0175	0.028± 0.006	0.032± 0.020	1.566± 0.144	1.83± 0.25	3.76± 0.37
27		13:04 - R	0.2600± 0.0177	0.036± 0.006	0.031± 0.020	1.775± 0.143	1.87± 0.24	3.37± 0.36
29		13:56 - R	0.3859± 0.0175	0.066± 0.006	0.058± 0.021	2.541± 0.143	2.59± 0.22	2.00± 0.39
23		11:38 - L	0.4195± 0.0174	0.068± 0.007	0.068± 0.021	2.618± 0.143	2.82± 0.22	1.67± 0.39
25		12:23 - L	0.2734± 0.0173	0.040± 0.007	0.030± 0.020	1.697± 0.144	1.90± 0.25	3.53± 0.37
27		13:04 - L	0.2672± 0.0173	0.037± 0.006	0.031± 0.020	1.763± 0.143	1.94± 0.27	3.43± 0.37
29		13:56 - L	0.3837± 0.0173	0.070± 0.006	0.056± 0.021	2.274± 0.143	2.42± 0.32	2.31± 0.46

Table 5-2 : Offline measurements and calculated species concentrations based on PLS models

			Offline measurements			Calculated concentrations based on Raman PLS predictions	
			Column 7	Column 8	Column 9	Column 10 = (column 1-11)	Column 11 = (column 2+3+4)
Run no:	Day	Time (L=lean; R= rich)	pH	Total MEA (w/w%)	CO_2 (mol / mol MEA)	Molecular CO_2 (mol / mol MEA)	Sum of carbon species (mol / mol MEA)
1	Day 1	11:41 - R	10.1	38.6	0.3286	-0.001	0.333
3		12:02 - R	9.8	40.2	0.3593	0.029	0.383
6		12:43 - R	9.7	27.5	0.5754	0.033	0.396
1		11:41 - L	10.5	38.8	0.2258	0.016	0.209
3		12:02 - L	10.5	38.6	0.2232	0.048	0.188
6		12:43 - L	10.5	39.7	0.2682	0.057	0.202
8	Day 2	11:37 - R	10.3	32.3	0.2303	0.008	0.226
10		12:06 - R	10.0	33.7	0.4451	0.080	0.326
12		12:37 - R	9.8	33.4	0.3952	0.136	0.308
8		11:37 - L	10.4	32.7	0.2618	0.272	0.005
10		12:06 - L	10.3	33.0	0.2730	-0.019	0.304
12		12:37 - L	10.2	33.6	0.3063	0.018	0.290
14	Day 3	11:55 - R	9.9	34.0	0.3972	0.015	0.383
16		12:27 - R	10.3	33.7	0.3010	0.041	0.270
18		12:57 - R	10.3	34.1	0.2756	0.012	0.273
20		13:26 - R	9.8	35.2	0.3974	0.379	0.004
14		11:55 - L	9.8	37.2	0.3958	0.027	0.395
16		12:27 - L	10.3	33.9	0.2684	0.216	0.065
18		12:57 - L	10.4	34.6	0.2514	0.013	0.248
20		13:26 - L	9.7	36.1	0.4392	0.028	0.408
23	Day 4	11:38 - R	10.1	35.8	0.3534	0.005	0.338
25		12:23 - R	10.4	35.0	0.2510	0.001	0.222
27		13:04 - R	10.4	35.8	0.2610	0.003	0.257
29		13:56 - R	9.9	37.6	0.4020	0.026	0.360
23		11:38 - L	9.8	36.7	0.4122	0.047	0.372
25		12:23 - L	10.4	36.4	0.2742	0.032	0.242
27		13:04 - L	10.4	36.9	0.2640	0.016	0.251
29		13:56 - L	9.7	39.2	0.5048	0.055	0.328

3.2. CO2 absorption profiles with time

Observation of CO2 absorption with time is an important aspect to understand the CO2 removal efficiency, absorption rate and the impact of process conditions to the absorber performance. Raman analyser was configured to collect data with total exposure time of 1 minute during this study. Therefore fast responses as well as numerous predictions were obtained during a total run time of couple of hours. Fig. 3-6 show how predicted CO2 loading evolve with time for four different days run time (given in Table 2). Offline titration results at some certain times are also presented in each graph for comparison.

Fig. 3 is related to run 1-6 where the gas flow rate in the rig was changed from 5 to 30 Nm³/h while keeping the liquid flow rate at 40 kg/h. Two channels of the Raman analyser were operated at the same time and hence lean and rich amine stream profiles could be observed simultaneously. Eventhough the gas flow rate was increased from time 11.41 to 12.43, a considerable change in CO2 concentration in both streams cannot be observed. Raman predictions for lean amine stream shows better fit with the titration results than the rich amine stream. This was assumed to be due to the more dynamic conditions at the rich stream measurement location. For all the other runs, only one channel of the Raman analyser was used and both rich and lean stream could not be monitored simultaneously (Fig. 4-6). Switching of the operating channel between two Raman probes (lean and rich amine streams) during the run time was performed instead.
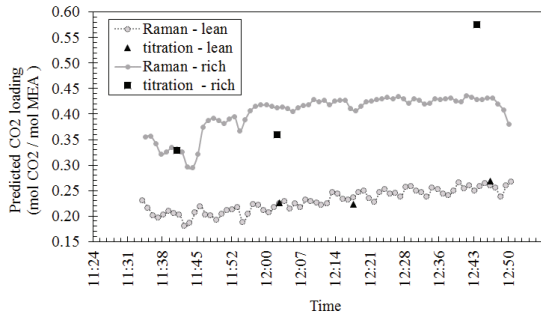
Fig. 3 : Comparison of titration and Raman predictions for CO2 loading (run 1-6)
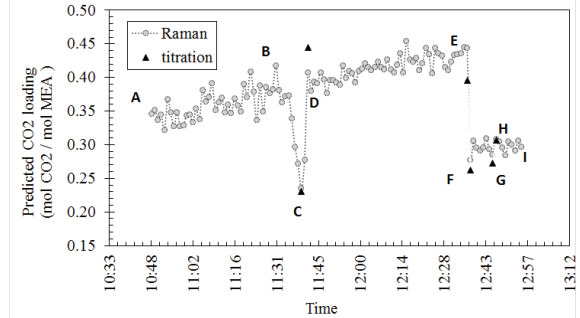
Fig. 4 : Comparison of titration and Raman predictions for CO2 loading (run 7-12)

Run 7-12 was monitored using one channel in the Raman analyser switching the channel between two streams time to time. According to Fig. 4, Point A-B , D-E and H-I are measurements from the rich stream. C and F-G are those for lean stream. During the time from B-C and E- F, Raman probe was transferred from rich to the lean amine stream and from C -D, it was transferred from rich to lean amine stream, so the predictions during these time intervals do not represent actual process stream variations. From time 11.03 to 12.37, the liquid circulation was decreased from 114 to 60 kg/h maintaining a gas flow rate at 30 Nm3/h. Titration measurements follow the trend of Raman predictions. Heavily fluctuating CO2 concentration in adjacent time intervals is an indication of the instability of the process.

Run 13-21 and 22-30 represent two sets of replicate experiments with similar process conditions of gas and liquid flow rates. According to Fig. 5 and 6, they have different initial CO2 concentrations in lean and rich amine streams.
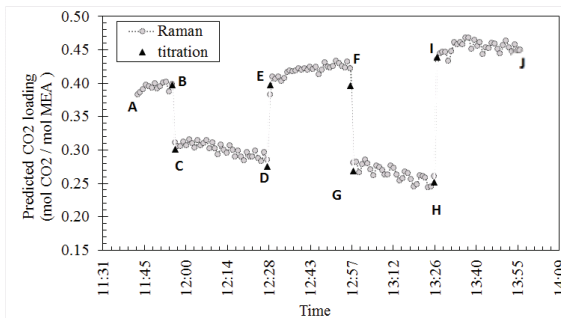

Fig. 5: Comparison of titration and Raman predictions for CO2 loading (run 13-21)
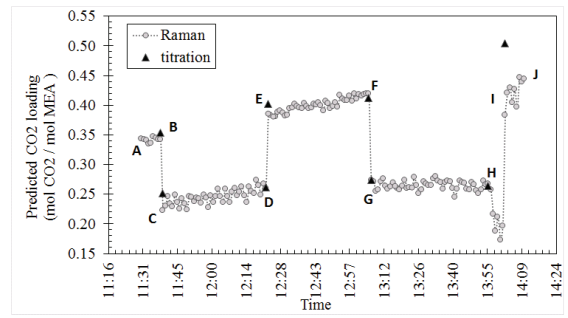
Fig. 6: Comparison of titration and Raman predictions for CO2 loading (run 22-30)

A-B, E-F and I-J are rich streams and C-D and G-H are lean streams. Good fit between predictions and titration measurements imply that the change in liquid flow rate from 112 to 30 kg/hr with time hasnot affected adversely to the predictability of the models. Rich stream shows increasing CO2 loading with time while the lean stream for run 13-21 has a decreasing CO2 content in lean stream as its initial value is higher than the minimum obtainable value for lean stream under this process conditions for the rig. For run 22-30, it shows that the lean stream has almost acquired this minimum level of concentration from the beginning and fluctuates around a same mean value with time. Time interval between each run on a certain day, was around 10-15 minutes and no investigation was done to check whether this allowance was enough to acquire maximum possible absorption/desorption by the unit. Therefore, no conclusions were made on the effect of different process variations to CO2 absorption / desorption rate

3.3. Demonstration of liquid concentration profiles

Results from the four demonstration cases are given in Table 3, are presented in this section to show how the models simultaneously predict CO2 loadings in lean and rich amine streams. Trials were performed after plugging two Raman channels to both streams and performing random variations in absorber inlet temperature, gas flow rate, liquid flow rate, regeneration conditions and CO2 percentage in flue gas. All cases started with the same CO2 content in lean and rich streams. Results are outlined in Fig. 7.


(a) Case 1

(b) Case 2

(c) Case 3

(d) Case 4
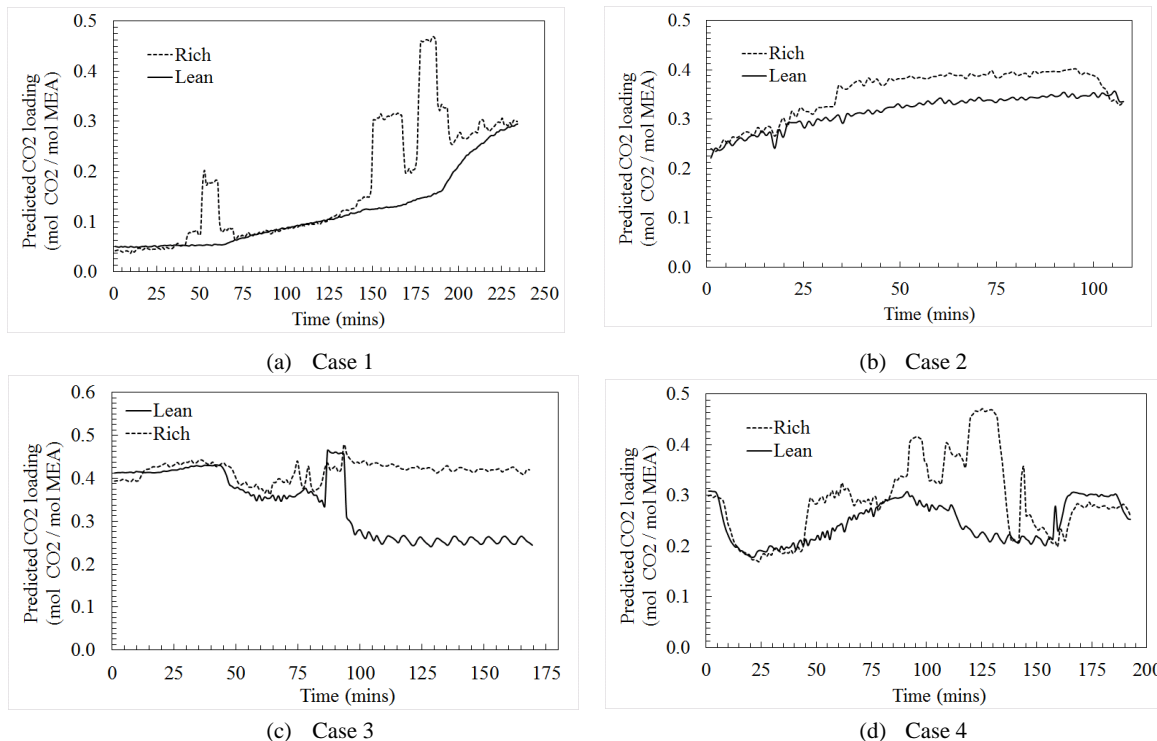
Fig. 7: Prediction of CO2 concentration in lean and rich amine streams amidst of different process conditions
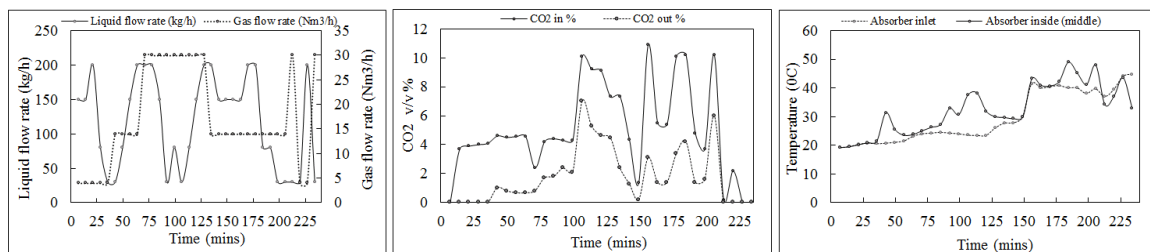
Fig. 8 : Changes of liquid and gas flow rates, CO2 percentage in flue gas stream and temperature in the absorber with time – Case 1

In Fig. 7 - Case 1 demonstrates the CO2 loading – PLS predictions when the rig was running without regeneration of the rich stream. Process conditions related to case 1 are presented in Fig. 8. In this trial, the absorber inlet temperature was increased gradually from 20^0C to 30^0C until 160 minutes. After that it was maintained with an average temperature of 40^0C until the end of the run. The fluctuations of CO2 concentration at some points can be correlated to changes in liquid flow rate, gas flow rate, absorber inlet/inside temperature and CO2 percentage in the flue gas stream with reference to information in Fig. 8. As an example, in rich stream, the increase in CO2 loading from 50 to 75 minutes was due to the changes of liquid to gas ratio (L/G) and between 150-175 minutes and 175-200 minutes was due to increase in CO2 % in inlet flue as stream.

Case 2 was aimed to monitor the steady state achievement with time when the flue gas flow rate and liquid flow rate were kept constant and absorber inlet was set to a fixed value. In this trial, gas flow rate was 14 Nm^3/h, liquid flow rate was 150 kg/h while absorber inlet temperature was 40^0C and CO2 content in the flue gas stream was 10-11%. Both lean and rich amine streams started with same CO2 level. Continuous CO2 supply to the absorber and favourable reaction temperature (40^0C) made the rich stream to have a higher absorption rate than the lean amine stream. After 97 minutes CO2 mixing to the flue gas was stopped which ended both rich and lean streams to reach an equalised in CO2 loading of 0.33 at the end of the run.

The effect of regeneration and liquid to gas ratio on the CO2 absorbed amine stream, can be visualized in Fig. 7-case 3. In this trial, CO2 percentage in the flue gas was maintained at 10-11%. There was no steam supply to the desorber upto 46 minutes. Since the initial CO2 level in both stream was higher than 0.39 mol CO2/mol MEA, upto 46 minutes the increase of CO2 level was very small. At 45 minutes, boiler in the desorber was started and it reached 120^0C by 75 minutes. As a result, the CO2 content in lean stream started to decrease. Simultaneously, rich stream CO2 content was also decreased as the L/G ratio was decreased from 150/14(kg/Nm^3) to 150/30(kg/Nm^3). At 85 minutes, change in L/G as 30/4(kg/Nm^3) resulted in a sudden peak in CO2 level in lean amine stream, however it ended up of final CO2 content of 0.227 mol CO2/mol MEA with time. Simultaneously, rich stream achieved a steady concentration level. In summary, Fig. 7 – case 3 is an example for the ability of the Raman online monitoring tool to observe the effect of regeneration and steady state operation conditions.

Case 4 describes the effect of CO2 volume fraction in the flue gas stream on the responses of lean and rich amine stream concentrations. Initially, both streams showed a loading of 0.29 mol CO2/ mol MEA. L/G ratio was 150/14(kg/Nm^3) but there was no CO2 in the gas flow and the desorber was operated with 120^0C boiler temperature. As a result of regeneration, CO2 was removed in the circulation liquid and reached a content of 0.178 mol CO2/mol MEA by 22 minutes. At 46 minutes, CO2 supply was started with 10% and again at 170 minutes, CO2 supply was stopped while L/G ratio was increased to 200/4(kg/Nm3). Both changes resulted to reach a CO2 content around 0.3 in lean and rich streams loading. Changes of other process conditions during 46 to 170 minutes, are not reported here. Based on the observations made during these demonstration cases, Raman signals gave ample opportunities to understand and monitor online concentration variations with respect to process dynamics in the system.

3.4. Prediction of species profiles

Based on the four test cases described in section 3.3, a complete speciation analysis was performed using 6 PLSR models. These species distribution curves with time can be used to understand which equilibrium chemical reactions

were affected most or least by different process conditions. Fig. 9 and 10 gives the plots for case 1 and 2, where it shows species distribution curves with respect to the CO2 loading for lean and rich streams. There is also a comparison of results with a theromodynamic equilibrium model data for 30% MEA at 40^0C calculated based on the Kent Eisenberg(KE) model [18]. To convert species concentrations in mol/L in KE model into mol/kg H2O at different CO2 loadings, densities available in [19] were used.


(a) rich stream   (b) lean stream
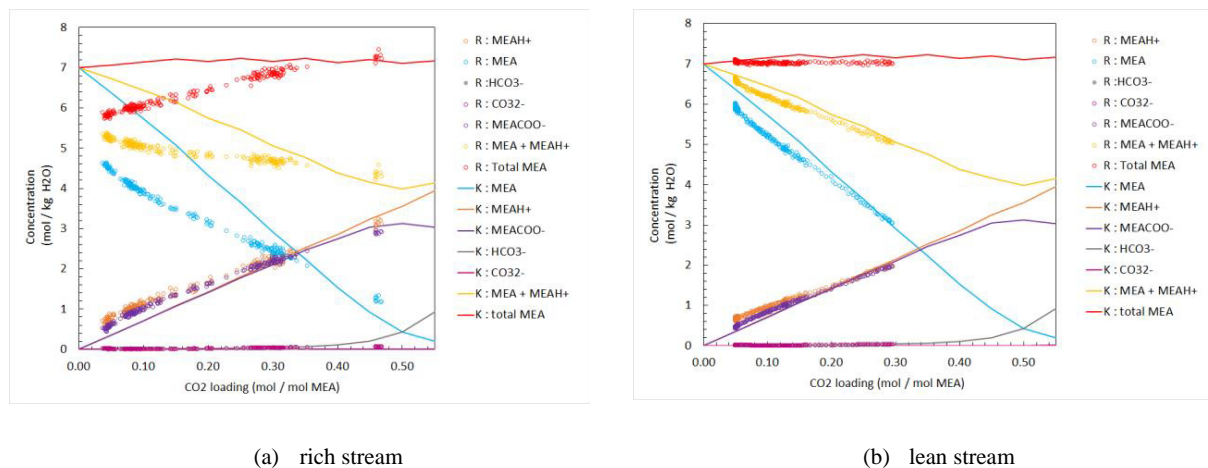
Fig. 9 : Species concentration against CO2-MEA molar loading – Case 1

According to Fig. 9-a, case 1 trial shows that Raman signals acquired from rich amine stream was sensitive to most of the process changes than the lean amine stream(Fig. 9-b). In case 1, there was no steam supply to the desorber. Eventhough the absorber inlet liquid temperature was maintained at a constant value, changes in process conditions resulted in different temperatures inside the absorber (refer table 2) which affected to the equilibrium species concentrations. Kent Eisenberg thermodynamic model represents the species distribution at a constant temperature and for a constant total amine concentration. Therefore a good match between the thermodynamic model (at 40^0C) and Raman predictions cannot be expected, specially for rich amine stream which only obtained 40^0C after 165 minutes of operation. Further, differences of total amine concentration between lean and rich amine streams at any specific time are indications of chemically unsteady state condition of the system.

(a) rich stream   (b) lean stream
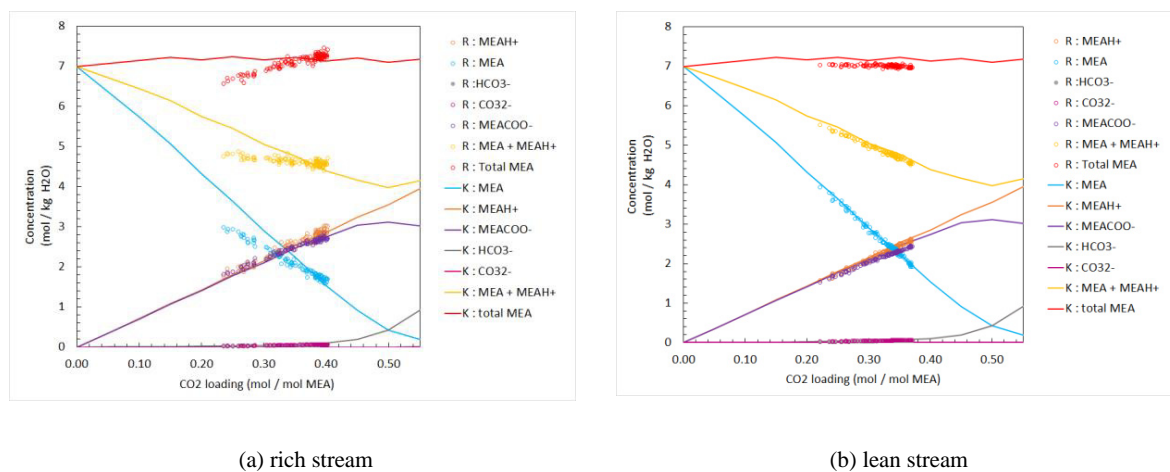
Fig. 10: Species concentration against CO2-MEA molar loading – Case 2

Fig. 10 is related to similar speciation analysis for case 2. According to the description given in section 3.3 for case 2, the aim of the trial was to monitor the speciation when process conditions were maintained at constant levels. Fig. 10-a implies that at lower CO2 loading values, the rich amine stream was not at steady conditions which was previously observed in Fig. 7-b. Fig. 7-b also claims that rich stream reached a reasonably steady state loading of 0.37 after 35 minutes. Raman predictions after 0.37 loading in Fig. 10-a also shows good fit with the Kent Eisenberg thermodynamic equilibrium model. Therefore there is an integrated match between information given by Fig. 7-b and 10-a. Lean amine stream (absorber liquid inlet) temperature and other process conditions were maintained at fixed values and therefore equilibrium conditions can be expected from the beginning of the trial in case 2-lean stream. This is proved based on the results in Fig. 10-b which reasonably match with the thermodynamic data.

4. Conclusion

In this study, the suitability of Raman spectroscopy combined with multivariate analysis methods was assessed to monitor online speciation of CO2 absorption process. Speciation predictions were based on six PLSR models developed for Raman spectroscopy. Total CO2 content predicted by the Raman PLS model was compared with offline titration analysis of the samples withdrawn during the measurement campaign. Titration measurements claimed a good alignment with predicted values. The ability of the models to cope with changing process conditions and the degree of predictability in equilibrium and non-equilibrium conditions were assessed using four demonstration cases. Speciation were compared with Kent Eisenberg thermodynamic model data and could logically explained. Based on this study, it was proved that Raman analyser is an efficient online process analytical tool to monitor liquid phase speciation in CO2 absorption process by MEA and gives fast and robust responses. However, it is recommended to perform offline ^{13}C NMR measurements to check the validity of predicted species concentration. The benefit of an online measurement tool for CO2 capture process is huge as they can be used to optimize process conditions, understand the chemistry in absorption process and abnormal functionalities in the plant as illustrated in this feasibility study. Integrating the Raman spectroscopy to the CO2 rig at USN, has now allowed more chance to explore the system operation with detailed understanding on absorption process.

Acknowledgement

References

[1] IEA, Technology roadmap carbon capture and storage in, International Energy Agency Paris, France, 2013.
[2] Alexander Kachko V M, Pauls Christoph, Stephan Hochgeschurz, Bathen Dieter ,Pasel Christoph, Bardow Andr, Speciation of MEA-H2O-CO2 by Raman spectroscopy :The impact of spectral analysis, in: 7th Trondheim CCS Conference, Trondheim, 2013.
[3] Geers L, Van De Runstraat A, Joh R, Schneider R, Goetheer E, Development of an Online Monitoring Method of a CO2 Capture Process, Industrial & Engineering Chemistry Research, 50 (2011) 9175-9180.
[4] Einbu A, Ciftja A F, Grimstvedt A, Zakeri A, Svendsen H F, Online analysis of amine concentration and CO2 loading in MEA solutions by ATR-FTIR spectroscopy at process conditions, Energy Procedia, (2012) 55-63.
[5] Souchon V, Aleixo M d O, Delpoux O, Sagnard C, Mougin P, Wender A, Raynal L, In situ determination of species distribution in alkanolamine- H2O - CO2 systems by Raman spectroscopy, Energy Procedia, 4 (2011) 554-561.
[6] Vogt M, Pasel C, Bathen D, Characterisation of CO2 absorption in various solvents for PCC applications by Raman spectroscopy, Energy Procedia, 4 (2011) 1520-1525.
[7] Wong M, Bustam M, Shariff A, Chemical speciation of CO2 absorption in aqueous monoethanolamine investigated by in situ Raman spectroscopy, International Journal of Greenhouse Gas Control, 39 (2015) 139-147.

[8] Alexandr Kachko L V v d H, André Bardow, Thijs J.H. Vlugt, Earl L.V. Goetheer, Comparison of Raman, NIR, and ATR FTIR spectroscopy as analytical tools for in-line monitoring of CO2 concentration in an amine gas treating process, International Journal of Greenhouse Gas Control, 47 (2016) 17-24.

[9] Kent R L, Eisenberg B, Better Data for Amine Treating, Hydrocarbon Process, 55 (1976) 87-90.

[10] Deshmukh R, Mather A, A Mathematical Model for Equilibrium Solubility of Hydrogen Sulfate and Carbon Dioxide in Aqueous Alkanolamine Solutions, Chemical Engineering Science, 36 (1981) 355-362.

[11] Austgen D, Rochelle G, Peng X, Chen C, Model of Vapor-Liquid Equilibria for Aqueous Acid Gas-Alkanolamine Systems Using the Electrolyte-NRTL Equation, Industrial Engineerign Chemistry, 28 (1989) 1060-1073.

[12] Socrates G, Alkane Group Residuals: C–H Group Infrared and RamanCharacteristic Group Frequencies: Tables and Charts, 3 ed., John Wiley & Sons Ltd, 2000.

[13] Batista De Carvalho L, Teixeira-Dias J, Raman spectra,conformational stability and normal coordinate analysis of ethylmethylamine, Journal of Raman Spectroscopy, 26 (1995) 653–661.

[14] Larkin P, in: Infrared and Raman Spectroscopy; Principles and Spectral Interpretation, Elsevier, 2011, pp. 73-115.

[15] Coates J, Interpretation of Infrared Spectra, A Practical Approach, in: Analytical Chemistry, John Wiley & Sons, Ltd., 2006.

[16] Tseng C-L, Chen Y-K, Wang S-H, Peng Z-W, Lin J-L, 2-Ethanolamine on TiO2 Investigated by in Situ Infrared Spectroscopy. Adsorption, Photochemistry, and Its Interaction with CO2, The Journal of Physical Chemistry A, 114 (2010) 11835-11843.

[17] Davis A R, Oliver B G, A vibrational-spectroscopic study of the speciespresent in the CO2-H2O system, Journal of Solution Chemistry, 1 (1972) 329–339.

[18] Øi L E, Removal of CO2 from exhaust gas, in, Telemark University College, Porsgrunn, 2012.

[19] Amundsen T G, Øi L E, Eimer D A, Density and Viscosity of Monoethanolamine + Water + Carbon Dioxide from (25 to 80) °C, Journal of Chemical & Engineering Data, 54 (2009) 3096-3100.